

**Ultrafast switching in a synthetic antiferromagnetic magnetic random-access memory device**Anders Bergman,<sup>1,2</sup> Björn Skubic,<sup>2</sup> Johan Hellsvik,<sup>2</sup> Lars Nordström,<sup>2</sup> Anna Delin,<sup>1,2,3</sup> and Olle Eriksson<sup>2</sup><sup>1</sup>*Department of Materials Science and Engineering, School of Industrial Technologies and Management, KTH, SE-10044, Stockholm, Sweden*<sup>2</sup>*Department of Physics and Astronomy, Uppsala University, Box 516, SE-75120, Uppsala, Sweden*<sup>3</sup>*Swedish e-Science Research Center, KTH, SE-10044, Stockholm, Sweden*

(Received 11 August 2010; revised manuscript received 9 April 2011; published 30 June 2011)

The dynamics of a synthetic antiferromagnet (a metallic trilayer) have been explored and are shown to exhibit ultrafast switching on a time scale of tens of ps. This conclusion is based on first-principles, atomistic spin dynamics simulations. The simulations are performed at finite temperature, as well as at  $T = 0$  K (the macrospin limit), and we observe a marked temperature dependence of the switching phenomenon. It is shown that, to reach very high switching speeds, it is important that the two ferromagnetic components of the synthetic antiferromagnet have oppositely directed external fields to one another. Then a complex collaboration between precession switching of an internal exchange field and the damping switching of the external field occurs, which considerably accelerates the magnetization dynamics. We discuss a possible application of this fast switching as a magnetic random access memory device, which has as a key component intrinsic antiferromagnetic couplings and an applied Oersted field.

DOI: [10.1103/PhysRevB.83.224429](https://doi.org/10.1103/PhysRevB.83.224429)

PACS number(s): 75.78.-n, 75.50.Ee, 75.50.Ss, 75.75.-c

**I. INTRODUCTION**

The microscopic mechanisms behind magnetization dynamics in different materials have recently raised interest both experimentally and theoretically. For instance, it has been found that a laser pulse can be used to demagnetize a ferromagnetic (FM) sample on time scales of 100 fs. This has led to research in what is now referred to as ultrafast demagnetization<sup>1–5</sup> where it is the relaxation of the electron spin in the exchange field which determines the switching speed. These studies are on a very fundamental level, and for practical aspects in magnetic recording media, it can be argued that a setup involving a laser might be a hinder. Nevertheless, several basic scientific questions are raised from these kinds of studies, and new forms of switching have been discussed, e.g., the recently proposed momentum induced switching where an analogy between the magnetic moment and the momentum of a classical particle has been drawn.<sup>5</sup>

Apart from being of fundamental interest, magnetization dynamics is of relevance in technology, especially in applications where magnetism is used to store information. Writing and retrieving information at ever higher speeds are demanded, and often this involves the switching dynamics of magnetic elements in a hard-disc or in a magnetic random access memory (MRAM). In the present study we investigate the magnetization dynamics of antiferromagnetic (AFM) structures, since it has been noted that switching processes can be made orders of magnitude faster than for conventional switching in ferromagnetic materials. AFM structures, where the magnetic order is changed through a thermally assisted change in the anisotropy field have been studied in Ref. 6. The present paper reports on a theoretical simulation of the dynamics of a synthetic antiferromagnet (a magnetic trilayer), and our primary interest is to obtain information on an atomic level, of the magnetization dynamics of such a system. However, we take the opportunity here to suggest how the dynamics of such a synthetic antiferromagnet can be used in a device.

Before entering the details of our theoretical method and the results, we make a short note on the current state of affairs as concerns magnetization dynamics and its connection to applications in devices. In a regular switching of a ferromagnet with the field antiparallel to the moment, the switching is driven by a precession and damping torque on the magnetization, a process which takes several nanoseconds.<sup>7</sup> A more efficient switching is obtained by utilizing the torque as is done in precession switching,<sup>8</sup> where the external field is applied perpendicularly to the magnetization. The fundamental limit of precession switching in a FM is directly related to the precession frequency of the FM in the external field and thereby to the strength of the external field.

Further avenues to improve on the write speed have been explored, such as the so-called “Toggle MRAM,”<sup>9</sup> the thermally assisted switching technique<sup>10</sup> as well as the spin-transfer torque technology.<sup>11</sup> The times achieved in these switching modes vary from a few nano-seconds<sup>10</sup> to sub-nanoseconds.<sup>12</sup> A review of these different switching modes may be found in Ref. 13.

In this article, we propose to utilize fast switching behavior of a synthetic antiferromagnetic structure,<sup>14</sup> which involves a magnetic heterostructure geometry with ferromagnetic units, which are separated by a nonferromagnetic interlayer. The latter layer provides an antiferromagnetic coupling of the ferromagnetic units, via the interlayer exchange coupling which can be tuned to be antiferromagnetic. We demonstrate that the synthetic antiferromagnet exhibits switching times of less than 20 ps. The switching process differs from “Toggle” or “Savtchenko switching”<sup>9</sup> utilized in modern MRAM devices, where antiferromagnetic heterostructures are used for achieving a toggle mode where an identical series of switching fields are used for switching both from one state to the other and back. In the structure we propose here, the AFM coupling is instead used for driving a fast switching mechanism which is analyzed in detail.

The synthetic antiferromagnet can be used in a device, which we would also like to propose here. The geometry of

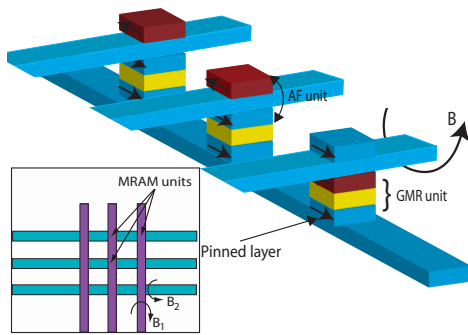


FIG. 1. (Color online) Schematic figure of an MRAM device utilizing antiferromagnetic exchange coupling. The bit line is the uppermost line in the figure, and generates an Oersted field,  $B$ . The digit line is the lowermost line. The magnetic units are represented by rectangular boxes, colored in red/dark grey (for magnetization direction into the figure) and blue/grey (for magnetization direction out of the figure). The GMR unit is represented by the blue, yellow (white) and red boxes, whereas the AF unit is represented by the red and blue boxes, separated by the bit line. An entire stack of GMR and AF unit is referred to as an MRAM unit. In order to achieve selectivity in switching of individual MRAM units a second bit line is needed as shown in the inset of the figure, where a top view of the device is shown. The second bit line is parallel to the digit line but placed in the vicinity of the AF unit. The second bit line is shown in purple (dark grey). The two bit lines give rise to magnetic fields  $B_1$  and  $B_2$ , respectively, and the requirement that their sum results in a total field which is oppositely directed for the two magnetic layers of the AF unit, but with the same magnitude for these layers.

this device is shown in Fig. 1. The stored binary code is carried by the resistance through a pillar consisting of two magnetic layers separated by a nonmagnetic spacer layer which provides a substantial GMR (giant magnetoresistance) effect.<sup>15,16</sup> This part of the device is referred to as the “GMR unit” in the following discussion. Only the top layer of the GMR unit has its magnetization reversed when a pulse is sent through the top lead, the bit line. The magnetic layer close to the bottom lead is pinned. A magnetic layer is also positioned on top of the top lead, and the geometry is here chosen so that there is a strong antiferromagnetic coupling between the magnetic element over the bit line and the layer just below the top lead. We will refer to this antiferromagnetic structure as the “AFM unit,” and it is this unit we focus on in this paper, since it is here the detailed aspects of magnetization dynamics are of importance. The functionality of the device in Fig. 1 is such that if a current is sent through the top leads (the two bit lines shown in Fig. 1), an Oersted field from each line ( $B_1$  and  $B_2$  in the inset of Fig. 1) is generated and in this way one can generate fields that switch one particular unit to have the lowest magnetic layer of the AFM unit being parallel or antiparallel to the lowest, pinned layer of the GMR unit. By measuring the magnetoresistance of the GMR unit one may detect the binary information stored. Two bit lines are needed to ensure selectivity in switching of individual MRAM units, and as shown in the inset of Fig. 1, where a top view of the device is shown, they are aligned in perpendicularly.

The purpose of the AFM unit is as discussed above, to provide an antiferromagnetic coupling in a system which has the potential of switching extremely fast. The question is only “how fast?” We have addressed this issue by means of first principles, atomistic spin dynamics simulations.<sup>17</sup> This method was originally suggested by Antropov *et al.*,<sup>18</sup> and until now only a handful simulations using it have been published.<sup>19–21</sup> The results presented here are obtained by a recently developed Atomistic Spin Dynamics (called UppASD) program package [<http://www.fysik.uu.se/cmt/asd>].<sup>17</sup> With this technique one does not have to rely on a macrospin model, instead the individual atomic spins evolve in time,<sup>22</sup> as a function of an external applied field, in particular when the simulations are made at finite temperature. For the numerical integration of the LLG equation the method of Ref. 23 was used.

Self-consistent electronic structure calculations are performed to obtain magnetic moments as well as interatomic exchange interactions for use in the SD simulations, and have been made by means of the Korringa-Kohn-Rostocker (KKR) Green’s function method within the atomic sphere approximation (ASA). The ground state electronic structure is mapped onto a Heisenberg Hamiltonian using the Liechtenstein-Katsnelson-Gubanov method (LKGM).<sup>24,25</sup> As a model of the central component of the device in Fig. 1, we chose two Fe units which are antiferromagnetically coupled in a sandwich geometry as follows:  $\text{Fe}_3/\text{Cr}_4/\text{Fe}_3$ . In our calculations we considered Cr as the mediator of the antiferromagnetic exchange interaction, since the strength of this antiferromagnetic coupling is known in the literature.<sup>26</sup> We note however that different solutions to obtain an AF unit are possible, for instance a nonmagnetic bit line which is clad with a magnetic layer with a uniform magnetization density. In practical realizations of the device illustrated in Fig. 1, one will most likely explore several such avenues, in particular also to accommodate thick enough layers of the bit line to enable currents which generate a sufficient Oersted field. We have not addressed these issues further in this model study, but focus rather on discussing which physical mechanisms enable a fast magnetization switching.

In our simulations, interatomic exchange parameters were calculated for all atoms within nine lattice spacings from each other. We found 3136  $k$ -points sufficient for convergence of the interatomic exchange parameters. The calculations show that whereas the nearest neighbor and next nearest neighbor exchange interactions dominate the interatomic exchange, at the same time the more long-ranged exchange interactions are by no means negligible. For instance, the nearest neighbor interaction between Fe atoms, is between an interface atom and an atom in the middle of the Fe film, and this interaction is calculated to be 1.8 mRy. There are two next-nearest interactions, between Fe atoms at the interface and between Fe atoms in the middle of the film. For the former, the interaction is 0.73 mRy and for the latter it is 0.19 mRy. The nearest neighbor Fe-Cr interaction is calculated to be antiferromagnetic with a strength of the exchange of  $-0.10$  mRy. The nearest neighbor Cr-Cr interaction is  $-0.28$  mRy.

The combination of first principles calculations and atomistic spin-dynamics simulations enable a theoretical treatment in which all parameters are calculated, and no experimental input as regards the size of the magnetic moments or the

exchange interactions are needed. In the simulations we have assumed the external field to be in the 0.1 mT–1 T range, i.e., field strengths that are realistic in a laboratory environment. In the spin-dynamics simulations, a rather small unit cell of 10 atoms in the simulation box was seen to be sufficient for 0 K simulations since this is the macrospin limit. For finite temperatures, we used a much larger cell size with 36000 atoms. As a means of testing convergence, we also performed simulations with 64000 atoms in the cell, resulting in no significant differences compared to the 36000-atom cell.

## II. RESULTS

### A. 0 K data

We now turn to the details of the dynamics of the synthetic antiferromagnet; the AFM unit in Fig. 1. A switching process of this unit is mimicked by simulating the response to applying two oppositely directed static external fields to the AFM unit, one field to each Fe layer, oppositely directed to the magnetization. The fact that the two ferromagnetic units in Fig. 1 have external fields that are oppositely directed to one-another, is a result of the special geometry considered here. In Fig. 2 we present the evolution of the components of the average magnetization for one of the Fe layers in the trilayer during the switching process. The  $x$  axis is in the out-of-plane direction. Note from the figure that we obtain a reversal time of 20–30 ps (see Fig. 2), which is more than one order of magnitude faster compared to the simulated switching time of a ferromagnetic system (data not shown).

In order to understand the rapid switching behavior of the synthetic antiferromagnet in Fig. 2 it is crucial to understand the interplay between the external fields and the internal exchange field in the AFM unit and the severe frustration

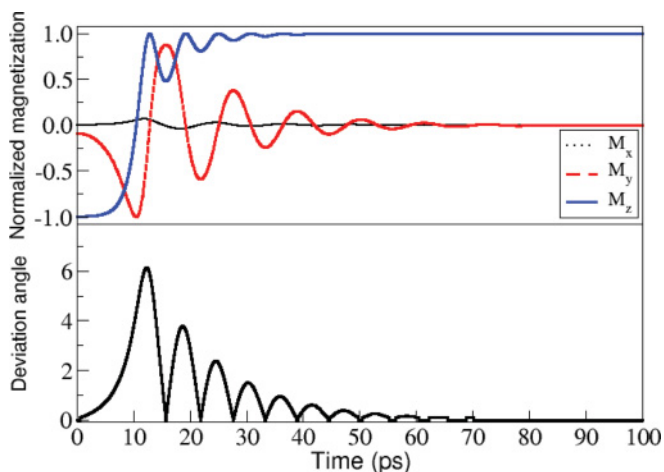


FIG. 2. (Color online) A simulation of the magnetization reversal of a  $\text{Fe}_3/\text{Cr}_4/\text{Fe}_3$  trilayer in an applied field of 0.1 T. The plot shows the time evolution of the components of the average magnetization of one of the Fe layers (top). The simulation is performed at 0 K with a damping constant of  $\alpha = 0.01$ . The magnetization is initially directed almost along the negative  $z$  direction ( $175^\circ$ ). In the bottom panel the deviation from 180 degree antiferromagnetic coupling between the two Fe slabs is shown (in degrees).

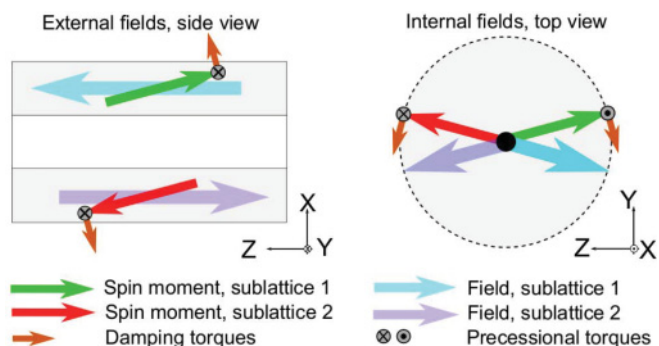


FIG. 3. (Color online) The left hand figure illustrates the torques exerted by an antiparallel external fields on the two sublattices of a synthetic antiferromagnet. Note the different directions of the external field for the two sublattices. The precessional torque gives rise to a frustration between the sublattices and an effective internal exchange field. The right hand figure illustrates a top view of the torques exerted by the internal exchange field. Damping torques from the external field and precessional torques from the exchange field bring the atomic moments to alignment with the external field.

between the AFM components of the structure that the external fields cause. To illustrate the complex switching phenomenon in the synthetic antiferromagnet, we consider the evolution of the magnetization of a synthetic antiferromagnet where the ferromagnetic layers have applied fields which are antiparallel to each other (which is what the Oersted field in Fig. 1 generates).

When the external field of the two sublattices are antiparallel (schematically shown in Fig. 3), a frustration results from the precessional torque on the two sublattices which counteract each other and build up an internal exchange energy as the angle between the magnetization deviates from  $180^\circ$  (shown in the bottom of Fig. 2). Meanwhile the damping torques on the two sublattices rotate the system uniformly toward the direction of the applied field. The growing internal exchange interaction results in two additional torques (shown to the right in Fig. 3). First, a damping component appears, which counteracts the precessional torque from the external Oersted field, and which slows down the growth of the internal exchange field. Second, a precessional torque develops, the action of which collaborates with the damping torque of the external field. Hence both the damping torque from the external field and the precessional torque from the internal exchange field assist in rotating the magnetization axis toward a new direction. This results in a very rapid switching.

For the synthetic AFM structure considered here, there is for a given external field an optimal damping parameter, which produces the lowest switching time. In Fig. 4 we present 0 K simulations for the  $\text{Fe}_3/\text{Cr}_4/\text{Fe}_3$  trilayer in a switching field of 100 mT for a range of damping parameters ( $\alpha = 0.001-1$ ). Note that in the figure we show a landscape of where switching has occurred, plotted as a function of damping parameter and time. In the so obtained phase diagram we can identify three ranges of  $\alpha$  with different switching behavior. In the low damping region ( $0.001 \leq \alpha \leq 0.01$ ), the damping torque in the internal exchange field is strong enough to balance off the precessional torque from the external field, but due to the rather



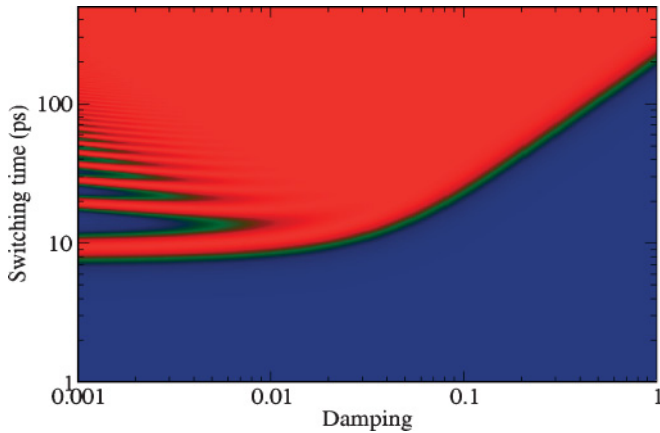


FIG. 4. (Color online) A switching diagram for the  $\text{Fe}_3/\text{Cr}_4/\text{Fe}_3$  system at 0 K. The phase diagram shows the  $z$  component of the average magnetization of one Fe layer color coded. The red/blue (light grey/dark grey) coloring indicates areas where switching has occurred/has not occurred. Three regions of damping are identified, corresponding to different switching dynamics—see text.

low value of the damping, this occurs when the angle between the magnetization of the layers has been reduced significantly. In a sense, a large reduction of the angle is desired since it leads to a large precessional torque on the magnetization from the internal exchange field. However, in the final relaxation phase of the switching process, the angle must be increased back to  $180^\circ$ . This final phase is in this case inhibited, leading to undesired switching oscillations, if the angle is reduced too much in the beginning of the switching process.

In the intermediate region ( $0.01 \leq \alpha \leq 0.1$ ), the value of the damping parameter and the external field strength are tuned with respect to each other and the interlayer coupling for an optimal switching process. In the strongly damped region ( $0.1 \leq \alpha$ ), the damping in the internal exchange field is large, which inhibits the initial reduction of the angle between the magnetization of the two layers. The precessional torque from the internal exchange field on the magnetization (which performs the rapid switching) is now small leading to a slow, mainly damping driven, switching. For optimal switching there is hence an optimal relationship between the AFM interlayer coupling, the damping and the magnitude of the external field. In this optimal situation, the damping torque is weak enough to allow the angle between the magnetization directions to become significantly less than  $180^\circ$ , but at the same time strong enough to result in fast relaxation back to a complete antiparallel configuration once the switching in the external field is finished.

In order to determine the influence of the external field to the time scale of the switching process, we have performed simulations for a large range of external fields, while keeping the damping parameter fixed. In Fig. 5 the dependence of the switching time as a function of applied field is shown. In these simulations, the damping was kept fixed to a value of  $\alpha = 0.05$ . Here we find that the switching times depend strongly on the external field which is consistent with our analysis of the switching mechanism, where the external field determines the strength of the internal field and both fields contribute to the switching process. As can be seen in Fig. 5,

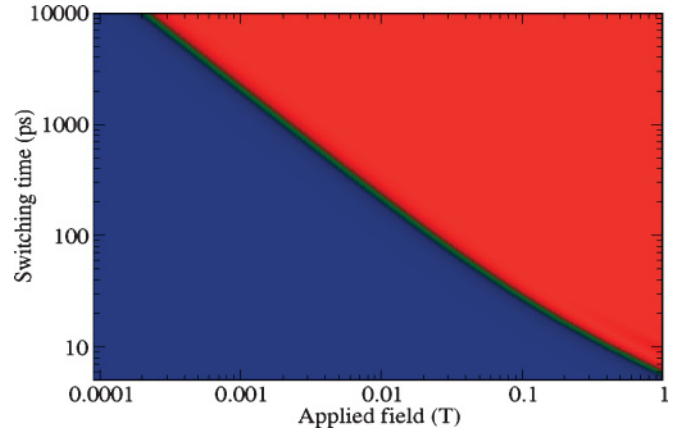


FIG. 5. (Color online) Switching time as a function of the applied field for the  $\text{Fe}_3/\text{Cr}_4/\text{Fe}_3$  system at 0 K. The phase diagram shows the  $z$ -component of the average magnetization of one Fe layer color coded. The red/blue (light grey/dark grey) coloring indicates areas where switching has occurred/has not occurred. The damping parameter was fixed to 0.05 for all fields.

switching times in the nanosecond regime are accessible for external fields in the mT range. At large external fields ( $\approx 1$  T) there is sign of an oscillation of the magnetization during the switching process. These oscillations have the same physical origin as the oscillations that were observed for the cases of very weak damping, which were shown in Fig. 4.

### B. Finite temperature effects

So far we have only considered switching behavior at 0 K, where all atomic spins co-rotate (i.e., a macrospin model). We now consider finite temperature effects in our simulations, and the results of these simulations are shown in Fig. 6. In the simulations shown in this figure we have used an optimal damping parameter, as identified in Fig. 4, i.e.,  $\alpha = 0.05$ . All parameters were otherwise the same as for the calculations shown in Fig. 4. For temperatures up to

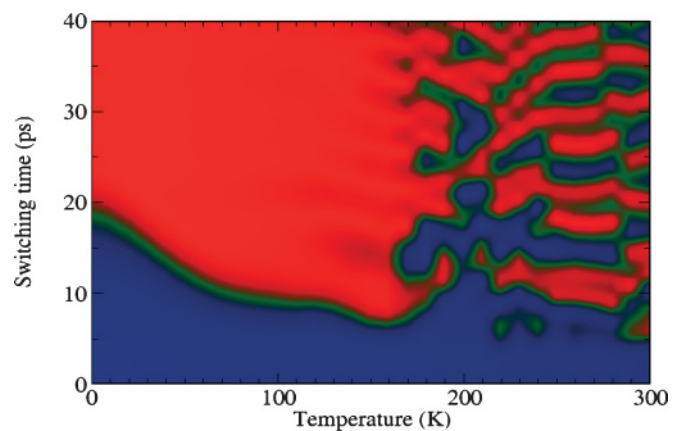


FIG. 6. (Color online) A switching diagram for the  $\text{Fe}_3/\text{Cr}_4/\text{Fe}_3$  system as a function of temperature. The phase diagram shows the  $z$  component of the average magnetization of one Fe layer color coded. The red/blue (light grey/dark grey) coloring indicates areas where switching has occurred/has not occurred.

150 K the switching process is well defined and is actually accelerated with increasing temperature. The explanation for this is that the thermal fluctuations tilt the individual magnetic moment in the ferromagnetic layers resulting in local internal fields that are not parallel to the magnetization of the whole layer. These deviations from perfect collinearity within the ferromagnetic layers provide a more suitable starting point for the switching once the external fields are turned on. The thermal fluctuations are however small enough to not influence the average magnetization of the layers and the switched system is stable for the whole simulation time.

At temperatures above 150 K the thermal fluctuations are so large that they start to dominate the dynamics of the system, resulting in a less defined switching scenario. At high temperatures there appears to be an oscillating behavior of the magnetization and while it may at first be suspected that this is due to strong disorder in the ferromagnetic layers, our simulations actually show that even for temperatures in the range of 300 K, there is still a well defined magnetization of the layers but the direction of the magnetization is fluctuating over time.

### III. CONCLUSION

In conclusion, by means of the suggested synthetic antiferromagnetic heterostructure, magnetization reversal on a time scale of tens of ps may be achieved by Oersted switching. This can be compared to switching times of order of nanoseconds in the ‘‘Savtchenko switching’’ mode.<sup>27,28</sup> In order to achieve these switching speeds, it is important that the two ferromagnetic components of the synthetic antiferromagnet

have oppositely directed external field to one another. Then a complex collaboration between precession switching of the exchange field and the damping switching of the external field occurs, which accelerates the magnetization dynamics. Our simulations also indicate that this switching should be stable at finite temperatures, although not at room temperature for the materials combination chosen in the present study.

The proposed switching mechanism provides an avenue for achieving very short reversal times, without having to rely on a technology based on a laser. Finally, the synthetic antiferromagnetic structure considered here may prove useful for systems with geometries where the shape anisotropy cannot be used to drive the magnetization dynamics (such as in perpendicular recording). Moreover, the suggested structure will have an advantage as sizes of magnetic bits are reduced to the point where the demagnetization field is reduced.

### ACKNOWLEDGMENTS

Financial support from the Swedish Foundation for Strategic Research (SSF), Swedish Research Council (VR), the Royal Swedish Academy of Sciences (KVA), the Carl Trygger Foundation, and Liljewalchs resestipendium is acknowledged. Calculations have been performed at the Swedish national computer centers UPPMAX, PDC, HPC2N and NSC under grants provided by the Swedish National Infrastructure for Computing (SNIC). O.E. is also grateful to the European Research Council (ERC) and the Knut and Alice Wallenberg Foundation for financial support. A.B. acknowledges support from eSENCE. Valuable discussions with Bernard Dieny are acknowledged.

<sup>1</sup>E. Beaurepaire, J.-C. Merle, A. Daunois, and J.-Y. Bigot, *Phys. Rev. Lett.* **76**, 4250 (1996).

<sup>2</sup>B. Koopmans, J. J. M. Ruijgrok, F. Dalla Longa, and W. J. M. de Jonge, *Phys. Rev. Lett.* **95**, 267207 (2005).

<sup>3</sup>K. Vahaplar, A. M. Kalashnikova, A. V. Kimel, D. Hinzke, U. Nowak, R. Chantrell, A. Tsukamoto, A. Itoh, A. Kirilyuk, and T. Rasing, *Phys. Rev. Lett.* **103**, 117201 (2009).

<sup>4</sup>J.-Y. Bigot, M. Vomir, and E. Beaurepaire, *Nature Physics* **5**, 515 (2009).

<sup>5</sup>A. V. Kimel, B. A. Ivanov, R. V. Pisarev, P. A. Usachev, A. Kirilyuk, and T. Rasing, *Nature Physics* **5**, 727 (2009).

<sup>6</sup>A. V. Kimel, A. Kirilyuk, A. Tsvetkov, R. V. Pisarev, and T. Rasing, *Nature (London)* **429**, 850 (2004).

<sup>7</sup>S. Tehrani, J. M. Slaughter, E. Chen, M. Durlam, J. Shi, and M. DeHerren, *IEEE Trans. Magn.* **35**, 2814 (1999).

<sup>8</sup>C. H. Back, D. Weller, J. Heidmann, D. Mauri, D. Guarisco, E. L. Garwin, and H. C. Siegmann, *Phys. Rev. Lett.* **81**, 3251 (1998).

<sup>9</sup>L. Savtchenko, B. N. Engel, N. D. Rizzo, M. F. Deherrera, and J. A. Janesky, U S Patent No. 6545906 (2003).

<sup>10</sup>J. Hérault, R. C. Sousa, C. Ducruet, B. Dieny, Y. Conraux, C. Portemont, K. Mackay, I. L. Prejbeanu, B. Delaët, M. C. Cyrille *et al.*, *J. Appl. Phys.* **106**, 014505 (2009).

<sup>11</sup>Y. Huai, F. Albert, P. Nguyen, M. Pakala, and T. Valet, *Appl. Phys. Lett.* **84**, 3118 (2004).

<sup>12</sup>H. Pham, D. Cimpoesu, A.-V. Plamadă, A. Stancu, and L. Spinu, *Appl. Phys. Lett.* **95**, 222513 (2009).

<sup>13</sup>J. M. Slaughter, *Annu. Rev. Mater. Res.* **39**, 277 (2009).

<sup>14</sup>S. Hernandez, M. Kapoor, and R. H. Victora, *Appl. Phys. Lett.* **90**, 132505 (2007).

<sup>15</sup>M. N. Baibich, J. M. Broto, A. Fert, F. Nguyen Van Dau, F. Petroff, P. Etienne, G. Creuzet, A. Friederich, and J. Chazelas, *Phys. Rev. Lett.* **61**, 2472 (1988).

<sup>16</sup>G. Binasch, P. Grünberg, F. Saurenbach, and W. Zinn, *Phys. Rev. B* **39**, 4828 (1989).

<sup>17</sup>B. Skubic, J. Hellsvik, L. Nordström, and O. Eriksson, *J. Phys. Condens. Matter* **20**, 315203 (2008) [<http://www.fysik.uu.se/cmt/asd/>].

<sup>18</sup>V. P. Antropov, M. I. Katsnelson, B. N. Harmon, M. van Schilfgaarde, and D. Kusnezov, *Phys. Rev. B* **54**, 1019 (1996).

<sup>19</sup>B. Ujfalussy, X.-D. Wang, D. M. C. Nicholson, W. A. Shelton, G. M. Stocks, Y. Wang, and B. L. Gyorffy, *J. Appl. Phys.* **85**, 4824 (1999).

<sup>20</sup>U. Nowak, O. N. Mryasov, R. Wieser, K. Guslienko, and R. W. Chantrell, *Phys. Rev. B* **72**, 172410 (2005).

<sup>21</sup>M. Fähnle, R. Drautz, R. Singer, D. Seiauf, and D. Berkov, *Comput. Mater. Sci.* **32**, 118 (2005).

<sup>22</sup>J. Hellsvik, B. Skubic, L. Nordström, and O. Eriksson, *Phys. Rev. B* **79**, 184426 (2009).

- <sup>23</sup>J. Mentink *et al.*, *J. Phys. Condens. Matter* **22**, 176001 (2010).
- <sup>24</sup>A. I. Liechtenstein, M. I. Katsnelson, and V. A. Gubanov, *J. Phys. F: Met. Phys.* **14**, L125 (1984).
- <sup>25</sup>A. L. Liechtenstein, M. I. Katsnelson, V. P. Antropov, and V. A. Gubanov, *J. Magn. Magn. Mater.* **67**, 65 (1987).
- <sup>26</sup>S. Mirbt, A. M. N. Niklasson, B. Johansson, and H. L. Skriver, *Phys. Rev. B* **54**, 6382 (1996).
- <sup>27</sup>B. N. Engel, J. Åkerman, B. Butcher *et al.*, *IEEE Trans. Magn.* **41**, 132 (2005).
- <sup>28</sup>S. A. Wolf, Lu Jiwei, M. R. Stan *et al.*, *Proc. IEEE* **12**, 2155 (2010).